INTERNATIONAL JOURNAL OF SYSTEMATIC AND EVOLUTIONARY MICROBIOLOGY

RESEARCH ARTICLE

Hezbri *et al.*, *Int. J. Syst. Evol. Microbiol.* 2024;74:006317

DOI 10.1099/ijsem.0.006317

MICROBIOLOGY SOCIETY

Blastococcus brunescens sp. nov., a member of the *Geodermatophilaceae* isolated from sandstone collected from the Sahara Desert in Tunisia

Karima Hezbri[1], Ikram kammoun[1], Imed Sbissi[2], Hans-Peter Klenk[3], Maria del Carmen Montero-Calasanz[4], Faten Ghodhbane-Gtari[1,5] and Maher Gtari[1,*]

Abstract

The taxonomic position of strain BMG 8361^T, isolated from sandstone collected in the Sahara Desert of Southern Tunisia, was refined through a polyphasic taxonomic investigation. Colonies of BMG 8361^T were pale-orange coloured, irregular with a dry surface and produced a diffusible pink or brown pigment depending on media. The Gram-positive cells were catalase-positive and oxidase-negative. The strain exhibited growth at 10–40 °C and pH values ranging from 5.5 to 9.0, with optima at 28–35 °C and pH 6.5–8.0. Additionally, BMG 8361^T demonstrated the ability to grow in the presence of up to 1% NaCl (w/v) concentration. The peptidoglycan of the cell wall contained *meso*-diaminopimelic acid, glucose, galactose, xylose, ribose, and rhamnose. The predominant menaquinones consisted of MK-9(H_4) and MK-9. The main polar lipids were phosphatidylcholine, phosphatidylinositol, glycophosphatidylinositol, diphosphatidylglycerol, phosphatidylethanolamine, and two unidentified lipids. Major cellular fatty acids were iso-$C_{16:0}$, iso-$C_{16:1}$ h, and $C_{17:1}$ ω8*c*. Phylogenetic analyses based on both the 16S rRNA gene and whole-genome sequences assigned strain BMG 8361^T within the genus *Blastococcus*. The highest pairwise sequence similarity observed in the 16S rRNA gene was 99.5% with *Blastococcus haudaquaticus* AT 7-14^T. However, when considering digital DNA–DNA hybridization and average nucleotide identity, the highest values, 48.4 and 86.58%, respectively, were obtained with *Blastococcus colisei* BMG 822^T. These values significantly undershoot the recommended thresholds for establishing new species, corroborating the robust support for the distinctive taxonomic status of strain BMG 8361^T within the genus *Blastococcus*. In conjunction with the phenotyping results, this compelling evidence leads to the proposal of a novel species we named *Blastococcus brunescens* sp. nov. with BMG 8361^T (=DSM 46845^T=CECT 8880^T) as the type strain.

INTRODUCTION

The genus *Blastococcus* [1] encompasses 15 species with validly published names sourced from diverse environments. *Blastococcus* species have been identified in habitats as varied as the seawater of the Baltic Sea (*Blastococcus aggregatus* [1]), monument samples (including *Blastococcus saxobsidens* [2], *Blastococcus capsensis* [3], *Blastococcus colisei* [4], *Blastococcus xanthinilyticus* [5], *Blastococcus tunisiensis* [6], and *Blastococcus carthaginensis* [7]), as well as desert soils and sands (with representatives such as *Blastococcus aurantiacus* [8], *Blastococcus haudaquaticus* [8], *Blastococcus mobilis* [8], *Blastococcus atacamensis* [9], and *Blastococcus deserti* [10]). While their ecological roles in these demanding conditions are still being unravelled, this recognition underscores their potential as valuable assets with significant biotechnological applications. These potential applications encompass various roles such as bioremediation, bioleaching, agriculture, enzyme production, and the generation of bioactive molecules [7, 11].

Author affiliations: [1]University of Carthage, National Institute of Applied Sciences and Technology, USCR Molecular Bacteriology and Genomics, Carthage, Tunisia; [2]Arid Regions Institute, LR Pastoral Ecology, Medenine, Tunisia; [3]Newcastle University, School of Natural and Environmental Sciences, Newcastle upon Tyne, UK; [4]IFAPA Las Torres-Andalusian Institute of Agricultural and Fisheries Research and Training, Junta de Andalucía, Seville, Spain; [5]University of La Manouba, Higher Institute of Biotechnology of Sidi-Thabet, Manouba, Tunisia.
***Correspondence:** Maher Gtari, maher.gtari@insat.rnu.tn
Keywords: diffusible brown pigment; *Geodermatophilaceae*; polyphasic taxonomy; stone-dwelling actinobacteria; taxogenomics.
Abbreviations: ANI, average nucleotide identity; dDDH, digital DNA–DNA hybridization; GYM, glucose–yeast extract–malt extract; ISP, International *Streptomyces* Project; ML, maximum-likelihood; MP, maximum-parsimony; R2A, Reasoner's 2A.
The GenBank accession numbers for the 16S rRNA gene and complete genome sequences for strain BMG 8361^T are LN626276 and CP141261, respectively.
Four supplementary figures and two supplementary tables are available with the online version of this article.

Strain BMG 8361^T was isolated as part of a research project focusing on the exploration of stone-dwelling actinobacteria in Tunisia. This strain demonstrated distinct phenotypic and genomic characteristics when compared to the type strains of validly named *Blastococcus* species. As a result, BMG 8361^T has been proposed as the type strain for a newly identified species named *Blastococcus brunescens* sp. nov.

ISOLATION AND MAINTENANCE

Strain BMG 8361^T was isolated from sandstone samples collected from the Sahara Desert in Tunisia, specifically located in Ong Jmal (34° 00′ 51″ N 7° 53′ 39″ E, Tozeur, Tunisia). The dust obtained from the 2–3 mm interior of the sandstone underwent serial dilution in a 0.85% saline solution. Aliquots from each dilution series were then plated on Luedemann medium (DSMZ medium 877) [12] and Reasoner's 2A (R2A) agar (DSMZ medium 830) [13], followed by incubation at 28°C for approximately 3 weeks. A predominant isolate, distinguished by its pale-orange colonies, underwent four successive subcultures on glucose–yeast extract–malt extract (GYM) *Streptomyces* medium (DSMZ medium 65). Pure cultures were preserved for long-term storage in glycerol stocks (35% w/v) at −80°C. These cultures have been deposited and are readily accessible at the Leibniz Institute DSMZ–German Collection of Microorganisms and Cell Cultures, as well as the Spanish Type Culture Collection, under the respective accessions DSM 46845^T and CECT 8880^T.

CULTURAL, MORPHOLOGICAL AND PHYSIOLOGICAL CHARACTERIZATION

Strain BMG 8361^T underwent an evaluation of its general cultural and morphological characteristics following a 15 day cultivation period at 28°C on various growth media. These encompassed (GYM) *Streptomyces* medium, R2A medium, Luedemann medium, complex medium 5006 (comprising sucrose 3 g l^{-1}, dextrin 15.0 g l^{-1}, meat extract 1.0 g l^{-1}, yeast extract 2.0 g l^{-1}, tryptone soy broth (Oxoid) 5.0 g l^{-1}, NaCl 0.5 g l^{-1}, K_2HPO_4 0.5 g l^{-1}, $MgSO_4$·7H2O g l^{-1}, $FeSO_4$·7H_2O 0.01 g l^{-1}), as well as International *Streptomyces* Project (ISP) 2, ISP5, and ISP7 media [14].

The growth temperature range of strain BMG 8361^T was investigated on GYM *Streptomyces* medium plates, covering temperatures from 5 to 45°C in 5°C increments. Modified ISP2 medium [14] was employed to assess growth under different pH conditions, with pH values ranging from pH 4.0 to 12.5 in 0.5 pH unit increments. Additionally, the response of the strain to diverse NaCl concentrations (0–10% w/v) was examined on yeast extract–malt extract medium (ISP2).

Key characteristics of BMG 8361^T were assessed using well-established procedures, including Gram-reaction analysis [15], examination of cell morphology with an optical microscope at 100-fold magnification and a field-emission scanning electron microscope, along with determination of oxidase and catalase activities (using 3% H_2O_2) [16]. Additionally, assessments included indole production, nitrate reduction, and hydrolysis of tyrosine [17], along with examinations of casein, starch, xanthine, hypoxanthine, and gelatin [18], as well as aesculin [19]. Further characterization involved the use of API ZYM strips (bioMérieux) and the Biolog GEN III identification systems, as previously described [3].

BMG 8361^T grew on all tested media. The colonies exhibited a pink-orange hue on GYM *Streptomyces*, showcasing irregularities with a dry surface. A diffusible pink pigment was observed on medium 5322 (ISP7), while a distinctive brown pigment was observed on medium 5006, a characteristic not reported for other *Blastococcus* type strains [2–10] (Fig. S1A, available in the online version of this article). Gram-positive cells displayed either ellipsoidal or rod-shaped morphology, existing as individual cells or forming three-dimensional coccoid aggregates. Single cells exhibited a rod-shaped structure (0.3–1.5×0.4–3.0 µm) or an ellipsoidal form (1.2–1.5×1.5–3.0 µm). Bud formation was observed for single cells. Coccoid aggregates, with a diameter of 1.2–2.5 µm, presented as linear, band-like, or column-like three-dimensional structures. Cells of diverse sizes and shapes were situated adjacent to each other (Fig. 1).

BMG 8361^T demonstrated growth at temperatures spanning from 10 to 40°C and within a pH range of pH 5.5–9.0, with optima at 28–35°C and pH 6.5–8.0. Additionally, it thrived in the presence of up to 1% NaCl. It exhibited positive reactions for xanthine degradation (Fig. S1B), similar to type strain of *B. xanthinilyticus* [5]. Negative reactions were observed for aesculin degradation, nitrate reduction, denitrification, indole production, and the degradation of casein, tyrosine, starch, gelatin, hypoxanthine, and arylamidase. Additionally, it tested negative for alkaline phosphatase, lipase esterase (C8), *α*-glucosidase esterase (C4), *α*-chymotrypsin, valine arylamidase, *β*-galactosidase, galactosidase, *α* and *β*-glucosidase, acid phosphatase, naphthol AS-BI-phosphohydrolase, lipase (C14), cystine arylamidase, trypsin, *β*-glucuronidase, *N*-acetyl-*β*-glucosaminidase, *α*-mannosidase, urease, and *α*-fucosidase. Strain BMG 8361^T did not grow in the presence of fusidic acid, minocycline, vancomycin, tetrazolium violet, and tetrazolium. The strain employed various substrates, including dextrin, maltose, trehalose, *β*-gentiobiose, sucrose, raffinose, melibiose, *N*-acetyl-D-glucosamine, D-glucose, D-fructose, D-fucose, L-rhamnose, D-sorbitol, D-mannitol, D-glucose-6-phosphate, L-glutamic acid, D-gluconic acid, D-glucuronic acid, quinic acid, *α*-ketoglutaric acid, potassium tellurite, tween 40, acetoacetic acid, and acetic acid. However, it did not utilize lactose, *N*-acetyl-neuraminic acid, D-mannose, D-serine, D-arabitol, troleandomycin, L-aspartic acid, L-histidine, lincomycin, guanidine hydrochloride, niaproof, D-galacturonic acid, and mucic acid. Distinctive features of strain BMG 8361^T and its close relatives are summarized in Table 1.

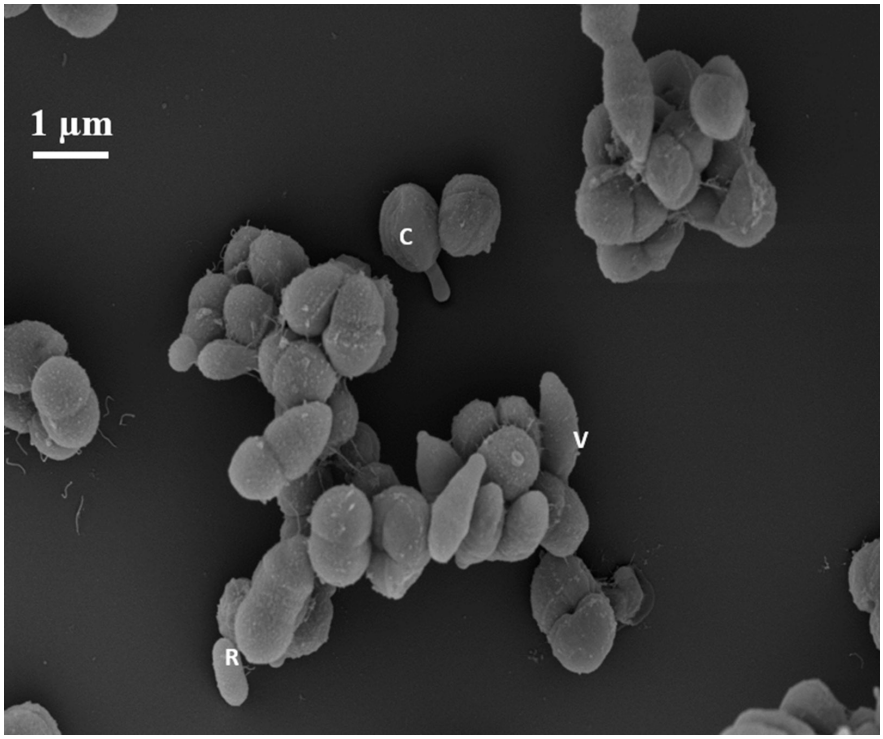

Fig. 1. Scanning electron microscopy was employed to capture the cellular morphology of strain BMG 8361^T, cultivated for 7 days on GYM *Streptomyces* medium at 28°C. The image highlights distinctive cell shapes, including cocci (c), rods (r), and vibrios (v).

CHEMOTAXONOMIC ANALYSES

Biomass of BMG 8361^T utilized for evaluating polar lipids, menaquinone, and whole-cell amino acids and sugars contents was acquired from 7-day-old culture in shake flasks containing liquid GYM *Streptomyces* medium at a temperature of 28°C until reaching the late exponential phase. Polar lipids were extracted and characterized through a two-dimensional thin-layer chromatography [20, 21]. Various spraying reagents were employed to reveal functional groups, including α-naphthol–sulphuric acid for the detection of sugar-containing lipids, Dragendorff's reagent (Merck) for the identification of choline-containing lipids [22], ninhydrin reagent (0.2% ninhydrin in acetone) for the revelation of amino groups [23], molybdenum blue (Sigma 119KG123) for the detection of lipids with phospho-groups, and finally 3.5% molybdatophosphoric acid (Merck) for the identification of total lipid content. Whole-cell amino acids and sugars were analysed following the protocols outlined by Lechevalier and Lechevalier [24] and Stanek and Roberts [25]. Menaquinones (MK) were assessed according to Collins *et al.* [26] and Kroppenstedt [27]. Peptidoglycan hydrolysates were assessed using the methods outlined by Schleifer and Kandler [28].

To analyse fatty acids, BMG 8361^T biomass was obtained following a 15 day culture on oligotrophic PYGV agar plates (DSMZ medium 621) at a temperature of 20°C [3]. Fatty acid analysis followed the approach detailed by Sasser [29]. Identification of fatty acids employed the MIDI System, Sherlock version 6.1, and the TSBA40 method with the ACTIN6 database.

Chemotaxonomic results indicated that the peptidoglycan composing the cell wall contained *meso*-diaminopimelic acid, along with glucose, galactose, xylose, ribose, and rhamnose as primary cell wall sugars. The predominant menaquinones present were MK-9 (H_4) and MK-9. The polar lipids included phosphatidylcholine, phosphatidylinositol, glycophosphatidylinositol diphosphatidylglycerol, phosphatidylethanolamine, and two unidentified lipids (Fig. S2). The cellular fatty acids were represented by iso-$C_{16:0}$ (39.6%), iso-$C_{16:1}$ h (20.1%), $C_{17:1}$ $\omega 8c$ (13.2%), $C_{18:1}$ $\omega 9c$ (5.2%), $C_{17:0}$ 10-methyl (4.8%), and iso-$C_{15:0}$ (4.2%) (Table S2).

PHYLOGENETIC AND TAXONOGENOMIC ANALYSES

Genomic DNA extraction from strain BMG 8361^T, cultivated in GYM *Streptomyces* broth at 28°C, was performed following the protocol outlined by William *et al.* [30]. DNA libraries for long-read sequencing were prepared using the Rapid sequencing gDNA-barcoding kit [SQK-RBK004, Oxford Nanopore Technologies (ONT)] and loaded onto the MinION SpotON flow cell (R9.4.1 FLO-MIN 106, ONT) without size selection. Sequencing was conducted on the MinION Mk1C device connected to MinKNOW version 22.05.8 for 48 h real-time base calling in high-accuracy mode using Guppy version 6.1.5 (quality score cut-off

Table 1. Phenotypic features of strain BMG 8361^T and its closely related type strains

Characteristic	BMG 8361^T	*Blastococcus colisei* BMG 822^T	*Blastococcus tunisiensis* BMG 823^T	*Blastococcus haudaquaticus* DSM 44270^T
Colony on GYM	Light rose orange	Coral	Pink orange	Reddish-brown coloured
Colony surface on GYM	Dry	Moist	Moist	Moist
Cell shape	Cocci, rods, vibrios	Cocci, rods, vibrios	Cocci, rods, vibrios	Cocci
Temperature range for growth (°C)	10–40	10–40	10–40	15–37
pH range for growth	5.5–9.0	6.0–10.0	5.5–9.0	5.0–11.0
NaCl for growth (%, w/v)	≤1	≤4	≤4	≤8
Production of:				
Alkaline phosphatase	–	+	–	–
Esterase (C4)	–	–	–	–
Esterase lipase (C8)	–	–	+	+
Leucine arylamidase	+	+	+	+
Valine arylamidase	–	+	–	+
Cystine arylamidase	–	+	–	+
α-Glucosidase	–	+	+	+
Lipase (C14)	–	–	–	+
Cell wall sugars	Gal, Glu, Xyl, Rib, Rham	Gal, Glu, Rib	Glu, Rib, Rham	Rib, Mann, Gal, Glu
Predominant menaquinones*	MK-9(H_4), MK-9	MK-9(H_4), MK-9, MK-9(H_2)	MK-9(H_4), MK-9	MK-9(H_4), MK-9(H_2), MK-8(H_4), MK-9, MK-9(H_6)
Phospholipids†	PC, PI, GPI, DPG, PE	DPG, PE, OH-PE, PC, PI, GPI	DPG, PE, PC, PI, GPI	DPG, PE, PG, PC, PI, GPI
Fatty acids‡	iso-$C_{16:0}$, iso-$C_{16:1}$ h, $C_{17:1}$cis9	iso-$C_{16:0}$, $C_{18:1}$cis9, $C_{17:1}$cis9, iso-$C_{16:1}$ h	iso-$C_{16:0}$, $C_{17:1}$cis9	iso-$C_{15:0}$, iso-$C_{16:1}$ h, iso-$C_{16:0}$, $C_{17:1}$ *ω8c*, $C_{18:1}$ *ω9c*, $C_{16:1}$ *ω7c*

+, Positive reaction; –, negative reaction; +/–, ambiguous; Gal, galactose ; Glu, glucose ; Rib, ribose ; Xyl, xylose ; Rham, rhamnose; MK, menaquinones; DPG, diphosphatidylglycerol; PE, phosphatidylethanolamine; OH-PE, hydroxy-phosphatidylethanolamine ; PG, phosphatidylglycerol; PC, phosphatidylcholine; PI, phosphatidylinositol ; GPI, glycophosphatidylinositol.
*Only components with ≥5% peak area ratio are presented.
†Components are listed in descending order of importance.
‡Only components with ≥10% peak area ratio are presented.

7). *De novo* assembly was conducted using the EPI2ME Labs platform (ONT) with the Flye version 2.8.1-b1676 assembler [31]. The resulting assemblies were polished using Racon version 1.4.16 [32] and Medaka version 1.5.0 (ONT; https://github.com/nanoporetech/medaka). The final polished genome was annotated using the NCBI Prokaryotic Genome Annotation Pipeline [33].

A single circular chromosome, encompassing a size of 4901425 bp, was assembled based on 1662424 reads (Table S1). The mean contig coverage reached 452, and the G+C content was determined to be 72.74mol%. The genomic annotation revealed the presence of 5678 protein-coding genes, 849 pseudogenes, three rRNA operons, and 48 tRNA genes.

In-depth taxogenomic analysis utilized the Type Strain Genome Server (https://tygs.dsmz.de/) [34] and closely related type strains from the List of Prokaryotic Names with Standing in Nomenclature (https://lpsn.dsmz.de) [35]. Pairwise genome sequence comparisons were computed, and intergenomic distances were determined using the 'trimming' algorithm and the d5 distance formula based on 100 distance replicates [36]. In parallel, a maximum-likelihood tree was generated involving rapid bootstrapping with the autoMRE criterion [37] followed by optimal tree search.

Digital DNA–DNA hybridization (dDDH) values and confidence intervals were calculated using the Genome-to-Genome Distance Calculator version 3.0 [38]. Pairwise 16S rRNA gene similarity and pairwise average nucleotide identity (ANI) were calculated at www.ezbiocloud.net/tools/ani [39].

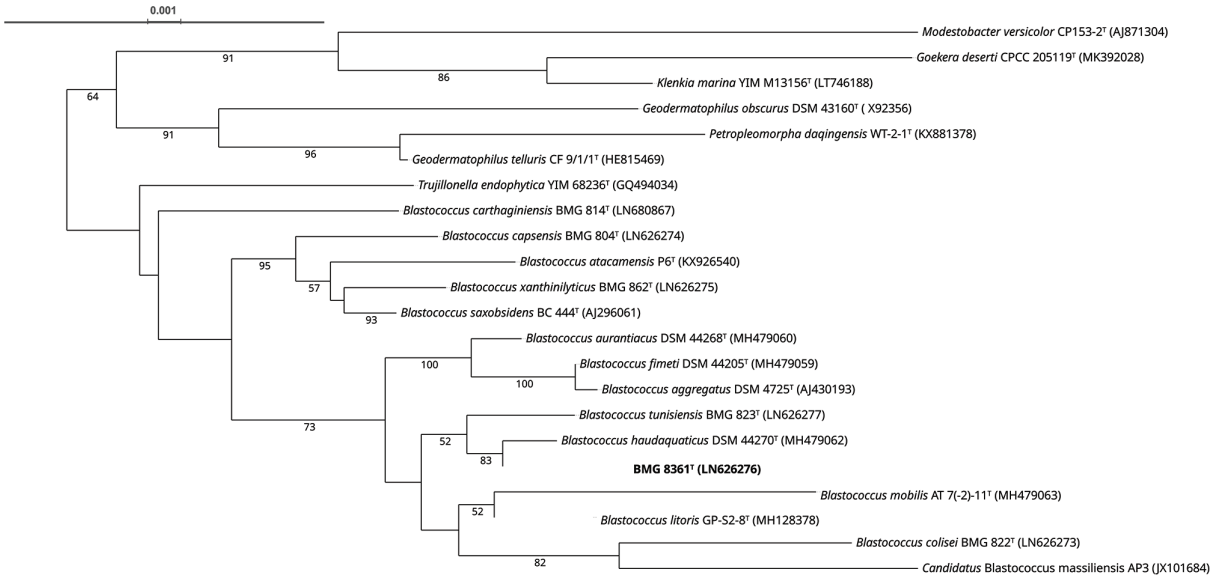

Fig. 2. The positioning of strain BMG 8361^T on the phylogenetic tree was established using the maximum-likelihood method for tree reconstruction based on 16S rRNA gene sequences. The generated maximum-likelihood tree employed the GTR+GAMMA model and was midpoint-rooted. Branch lengths on the tree reflect the anticipated number of substitutions per site. Numerical values above the branches indicate support levels, with values exceeding 60% obtained from both maximum-likelihood (on the left) and maximum-parsimony (on the right) bootstrapping. *Geodermatophilaceae* type strains served as the outgroups. The scale bar represents the evolutionary distance in substitutions per position.

Phylogenetically, strain BMG 8361^T emerges as a novel member of the family *Geodermatophilaceae* within the genus *Blastococcus* (Fig. S3), forming a subcluster with *B. haudaquaticus* AT 7-14^T and *B. tunisiensis* BMG 823^T (Fig. 2), which exhibited the highest calculated 16S rRNA gene similarities of 99.5 and 99.4%, respectively, with this new strain (Table 2). Whole-genome phylogenetic analysis confirmed the classification of BMG 8361^T, placing it within the same subcluster that includes *B. colisei* BMG 822^T, *B. tunisiensis* BMG 823^T, *B. haudaquaticus* DSM 44270^T, *B. litoris* GP-S2-8^T, and *B. mobilis* DSM 44272^T (Fig. 3). Consistently,

Table 2. Comparative analysis of 16S rRNA similarities, dDDH, and ANI values for BMG 8361^T with *Blastococcus* type strains

BMG 8361^T	**16S rRNA similarity**	**dDDH [CI]**	**ANI (%)**
Blastococcus colisei BMG 822^T (VFQE00000000)	97.98	48.4 [45.0–51.9]	86.58
Blastococcus tunisiensis BMG 823^T (FOND00000000)	99.41	47.8 [44.4–51.2]	86.18
Blastococcus haudaquaticus DSM 44270^T (OCNK00000000)	99.50	45.2 [41.8–48.7]	84.21
Blastococcus litoris GP-S2-8^T (QCZF00000000)	98.65	43.6 [40.3–47.1]	83.75
Blastococcus mobilis DSM 44272^T (FZNO00000000)	98.24	32.9 [29.5–36.4]	83.06
Blastococcus saxobsidens DSM 44509^T (SHKV00000000)	98.12	31 [27.7–34.6]	81.21
Blastococcus carthaginiensis BMG 814^T (JASNFN000000000)	97.34	29.5 [26.2–33.2]	81.13
Blastococcus xanthinilyticus BMG 862^T (VNHW00000000)	97.93	31.8 [28.5–35.4]	81.37
Blastococcus aggregatus DSM 4725^T (OBQI00000000)	98.88	29 [25.6–32.6]	81.42
Blastococcus fimeti DSM 44205^T (FNAW00000000)	98.95	30.4 [27.0–34.0]	81.12
Blastococcus atacamensis P6^T (POQU00000000)	97.89	29.6 [26.2–33.2]	80.90
Blastococcus capsensis BMG 804^T (JASNNW000000000)	98.34	29 [25.6–32.6]	80.94
Blastococcus aurantiacus DSM 44268^T (FNBT00000000)	98.87	30.2 [26.8–33.8]	80.91
Trujillonella endophytica DSM 45413^T (FOEE00000000)	97.63	24 [20.7–27.7]	79.39

[CI], confidence interval.

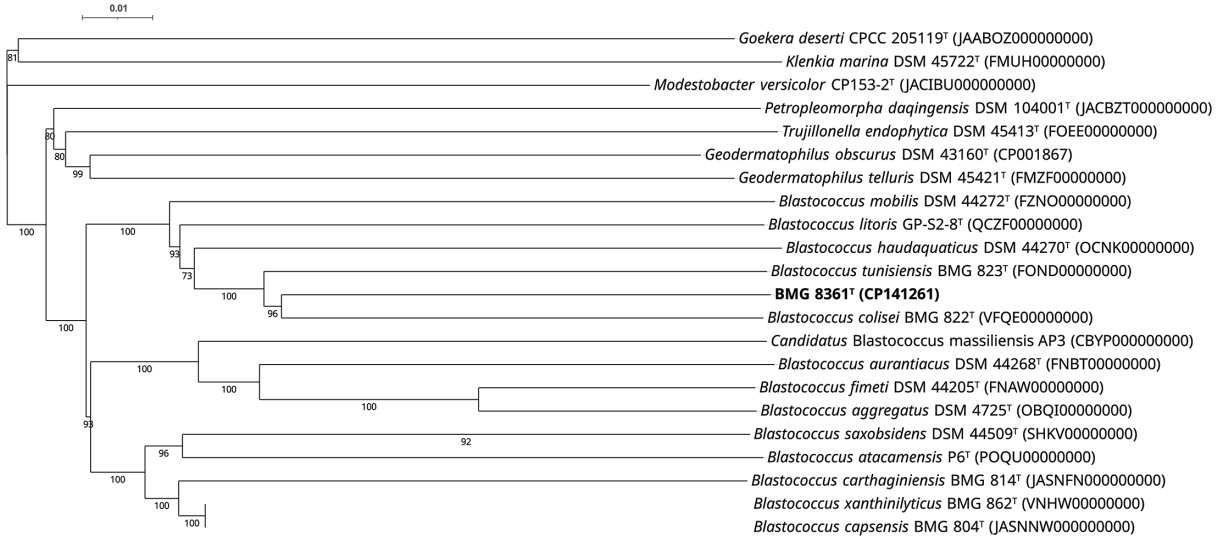

Fig. 3. The phylogenomic tree was generated utilizing FastME 2.1.6.1, relying on Genome-BLAST Distance Phylogeny (GBDP) distances computed from genome sequences of BMG 8361^T and closely related *Blastococcus* type strains. The branch lengths on the tree are proportional to the GBDP distance, calculated using the d5 formula. Numerical values above the branches represent GBDP pseudo-bootstrap support, consistently surpassing 60% across 100 replications, with an average branch support of 90.1%. The tree was midpoint-rooted, and *Geodermatophilaceae* type strains serving as outgroups. The scale bar denotes the evolutionary distance in substitutions per position.

the dDDH and ANI values of strain BMG 8361^T were obtained in descending order, aligning closely with *B. colisei* BMG 822^T, followed by *B. tunisiensis* BMG 823^T, and subsequently, *B. haudaquaticus* DSM 44270^T (Table 2). However, it was noteworthy that these dDDH and ANI values fell significantly below the commonly accepted prokaryotic species differentiation thresholds of <70 % and <95%, respectively [40–42].

GENOMIC PREDICTION OF ECOLOGICAL FEATURES AND SECONDARY METABOLITES

Blastococcus species have been identified as key components in soils facing diverse challenges, including dryness [2–11], salinity [43], alkalinity [44], exposure to toxins [45], and notably, heavy metal contamination [46–50]. Consequently, the distribution of genes associated with stress response, antibiotic resistance, as well as resistance to heavy metals and toxic compounds, were evaluated within these genomes. This assessment was conducted using the SEED server [51] following the annotation of genomes from strain BMG 8361^T and its closest phylogenomic type strains, *B. colisei* BMG 822^T, *B. tunisiensis* BMG 823^T, and *B. haudaquaticus* AT 7-14^T, accomplished through the Rapid Annotation Subsystem Technology server [52]. Results (Fig. S4) showed that in stress response mechanisms, BMG 8361^T demonstrated a robust profile in choline and betaine uptake and betaine biosynthesis under osmotic stress, suggesting its resilience in environments with varying osmotic pressures. On the other hand, *B. colisei* BMG 822^T displayed distinctive genomic characteristics in multiple stress-related subcategories, indicating specific adaptations to environmental challenges. For oxidative stress responses, bacterial haemoglobins, carbon starvation, and sigmaB stress response regulation, the strains collectively shared and diverged, emphasizing their diverse strategies in coping with stressors. For resistance to antibiotics and toxic compounds, BMG 8361^T exhibited unique patterns, with heightened activity in beta-lactamase and variations in resistance to vancomycin, fluoroquinolones, chromium compounds, cadmium, cobalt–zinc–cadmium, and copper homeostasis. The strain also displayed specific features in copper resistance proteins and multidrug resistance transporters, indicating its specialized adaptations to different metal stresses. In resistance to mercury compounds, BMG 8361^T showcased distinctiveness in mercuric reductase and the mercury resistance operon, suggesting a unique approach to dealing with mercury-related stress.

The remarkable adaptability and versatility displayed by *Blastococcus* species establish them as valuable entities with substantial biotechnological promise [53–55]. Consequently, the prediction of secondary metabolite biosynthesis gene clusters for strain BMG 8361^T, alongside its closest phylogenomic type strains, was conducted using antiSMASH [56] under both 'strict' and 'relaxed' settings (Fig. S3).

While all strains shared the production of loseolamycin A1/loseolamycin A2 (T3PKS) and isorenieratene (terpene), distinctions arose in NRPS-like, where BMG 8361^T and *B. tunisiensis* BMG 823^T synthesized stenothricin. Unique to *B. colisei* BMG 822^T was the production of ansacarbamitocin A (RRE-containing). In betalactone biosynthesis, BMG 8361^T and *B. colisei* BMG 822^T produced paramagnetoquinone 1/paramagnetoquinone 2, while *B. haudaquaticus* AT 7-14^T and *B. tunisiensis* BMG 823^T produced

corynecin III/corynecin. Importantly, BMG 8361^T lacked a redox-cofactor, in contrast to *B. tunisiensis* BMG 823^T. Furthermore, BMG 8361^T did not possess a phosphonate secondary metabolite, unlike *B. colisei* BMG 822^T.

In summary, our polyphasic taxonomic approach, integrating taxonogenomic data, firmly establishes BMG 8361^T as a distinct lineage within the genus *Blastococcus*. Therefore, we advocate for the formal recognition of BMG 8361^T (=DSM 46845^T=CECT 8880^T) as the type strain for a recently identified species, designated *Blastococcus brunescens* sp. nov.

DESCRIPTION OF *BLASTOCOCCUS BRUNESCENS* SP. NOV.

Blastococcus brunescens (bru.nes'cens. N.L. part. adj. *brunescens*, becoming brown, pertaining to the diffusible brown pigment produced by the type strain).

The colonies are pink-orange on GYM *Streptomyces*, irregular with a dry surface. Gram-reaction positive, coccoid, with a tendency to form coccoid aggregates, or ellipsoidal to rod-shaped with bud formation. Catalase-positive and oxidase-negative. A diffusible pink pigment is produced on medium 5322 (ISP 7), and a brown pigment is observed on medium 5006. Growth is observed within temperatures ranging from 10 to 40°C, with optimal conditions occurring at 28–35°C, and across pH levels ranging from pH 5.5 to 9.0, with pH optima between pH 6.5 and 8.0. Additionally, it thrives in environments containing up to 1% NaCl. Utilizes dextrin, maltose, trehalose, *β*-gentiobiose, sucrose, raffinose, melibiose, *N*-acetyl-D-glucosamine, D-glucose, D-fructose, D-fucose, L-rhamnose, D-sorbitol, D-mannitol, D-glucose-6-phosphate, L-glutamic acid, D-gluconic acid, D-glucuronic acid, quinic acid, *α*-ketoglutaric acid, potassium tellurite, Tween 40, acetoacetic acid, and acetic acid. However, it does not utilize lactose, *N*-acetyl-neuraminic acid, D-mannose, D-serine, D-arabitol, troleandomycin, L-aspartic acid, L-histidine, lincomycin, guanidine hydrochloride, niaproof, D-galacturonic acid, and mucic acid. Positive for xanthine degradation but negative for aesculin degradation, nitrate reduction, denitrification, indole production, and the degradation of casein, tyrosine, starch, gelatin, hypoxanthine and arylamidase but negative for alkaline phosphatase, lipase esterase (C8), *α*-glucosidase esterase (C4), *α*-chymotrypsin, valine arylamidase, β-galactosidase, galactosidase, *α* and *β*-glucosidase, acid phosphatase, Naphthol AS-BI-phosphohydrolase, lipase (C14), cystine arylamidase, trypsin, *β*-glucuronidase, *N*-acetyl-*β*-glucosaminidase, *α*-mannosidase, urease, and *α*-fucosidase. Does not grow in presence of fusidic acid, minocycline, vancomycin, tetrazolium violet, and tetrazolium. The peptidoglycan of the cell wall contains *meso*-diaminopimelic acid, glucose, galactose, xylose, ribose, and rhamnose. The predominant menaquinones are MK-9(H_4) and MK-9. The main polar lipids are phosphatidylcholine, phosphatidylinositol, glycophosphatidylinositol, diphosphatidylglycerol, phosphatidylethanolamine, and two unidentified lipids. The cellular fatty acids are mainly iso-$C_{16:0}$, iso-$C_{16:1}$ h and $C_{17:1}$ *ω*8c.

The type strain, BMG 8361^T (=DSM 46845^T=CECT 8880^T), was isolated from sandstone samples collected from the Sahara Desert in Tunisia, specifically located in Ong Jmal (34° 00′ 51″ N 7° 53′ 39″ E, Tozeur, Tunisia).

The GenBank accession numbers for the 16S rRNA gene and complete genome sequences for strain BMG 8361^T are LN626276 and CP141261, respectively.

Funding information
The authors received no specific grant from any funding agency.

Conflicts of interest
The authors declare that there are no conflicts of interest.

References

1. Ahrens R, Moll G. Ein neues knospendes Bakterium aus der Ostsee. *Archiv Mikrobiol* 1970;70:243–265.
2. Urzì C, Salamone P, Schumann P, Rohde M, Stackebrandt E. *Blastococcus saxobsidens* sp. nov., and emended descriptions of the genus *Blastococcus* Ahrens and Moll 1970 and *Blastococcus aggregatus* Ahrens and Moll 1970. *Int J Syst Evol Microbiol* 2004;54:253–259.
3. Hezbri K, Louati M, Nouioui I, Gtari M, Rohde M, *et al*. *Blastococcus capsensis* sp. nov., isolated from an archaeological roman pool and emended description of the genus *Blastococcus*. *Int J Syst Evol Microbiol* 2016;66:4864–4872.
4. Hezbri K, Nouioui I, Rohde M, Schumann P, Gtari M, *et al*. *Blastococcus colisei* sp. nov, isolated from an archaeological amphitheatre. *Antonie van Leeuwenhoek* 2017;110:339–346.
5. Hezbri K, Nouioui I, Rohde M, Spröer C, Schumann P, *et al*. *Blastococcus xanthinilyticus* sp. nov., isolated from monument. *Int J Syst Evol Microbiol* 2018;68:1177–1183.
6. Louati M, Hezbri K, Montero-Calasanz MDC, Rohde M, Göker M, *et al*. *Blastococcus tunisiensis* sp. nov., isolated from limestone collected in Tunisia. *Int J Syst Evol Microbiol* 2022;72.
7. Kammoun I, Hezbri K, Sbissi I, Del Carmen Montero-Calasanz M, Klenk H-P, *et al*. *Blastococcus carthaginiensis* sp. nov., isolated from a monument sampled in Carthage, Tunisia. *Int J Syst Evol Microbiol* 2023;73:006178.
8. Montero-Calasanz MDC, Yaramis A, Rohde M, Schumann P, Klenk H-P, *et al*. Genotype-phenotype correlations within the *Geodermatophilaceae*. *Front Microbiol* 2022;13:975365.
9. Castro JF, Nouioui I, Sangal V, Choi S, Yang SJ, *et al*. *Blastococcus atacamensis* sp. nov., a novel strain adapted to life in the Yungay core region of the Atacama Desert. *Int J Syst Evol Microbiol* 2018;68:2712–2721.
10. Yang ZW, Asem MD, Li X, Li LY, Salam N, *et al*. *Blastococcus deserti* sp. nov., isolated from a desert sample. *Arch Microbiol* 2019;201:193–198.

11. Essoussi I, Ghodhbane-Gtari F, Amairi H, Sghaier H, Jaouani A, *et al*. Esterase as an enzymatic signature of *Geodermatophilaceae* adaptability to Sahara desert stones and monuments. *J Appl Microbiol* 2010;108:1723–1732.
12. Luedemann GM. *Geodermatophilus*, a new genus of the *Dermatophilaceae* (Actinomycetales). *J Bacteriol* 1968;96:1848–1858.
13. Reasoner DJ, Blannon JC, Geldreich EE. Rapid seven-hour fecal coliform test. *Appl Environ Microbiol* 1979;38:229–236.
14. Shirling EB, Gottlieb D. Methods for characterization of *Streptomyces* species. *Int J Syst Bacteriol* 1966;16:313–334.
15. Gregersen T. Rapid method for distinction of gram-negative from Gram-positive bacteria. *European J Appl Microbiol Biotechnol* 1978;5:123–127.
16. Cross T. Growth and examination of actinomycetes-some guidelines. In: *Bergey's Manual of Systematic Bacteriology*, vol. 4. Springer, 1989. pp. 2340–2343.
17. Gordon RE, Smith MM. Proposed group of characters for the separation of *Streptomyces* and *Nocardia*. *J Bacteriol* 1955;69:147–150.
18. Clarke SK. A simplified plate method for detecting gelatine-liquefying bacteria. *J Clin Pathol* 1953;6:246–248.
19. Swan A. The use of a bile-aesculin medium and of Maxted's technique of Lancefield grouping in the identification of enterococci (group D streptococci). *J Clin Pathol* 1954;7:160–163.
20. Minnikin DE, O'Donnell AG, Goodfellow M, Alderson G, Athalye M, *et al*. An integrated procedure for the extraction of bacterial isoprenoid quinones and polar lipids. *J Microbiol Methods* 1984;2:233–241.
21. Kroppenstedt R, Goodfellow M. The family *Thermomonosporaceae*: *Actinocorallia*, *Actinomadura*, *Spirillispora* and *Thermomonospora*. In: *The Prokaryotes*, vol. 3. New York, NY, USA: Springer, 2006. pp. 682–724.
22. Tindall BJ. A comparative study of the lipid composition of *Halobacterium saccharovorum* from various sources. *Syst Appl Microbiol* 1990;13:128–130.
23. Skipski VP, Peterson RF, Barclay M. Quantitative analysis of phospholipids by thin-layer chromatography. *Biochem J* 1964;90:374–378.
24. Lechevalier MP, Lechevalier H. Chemical composition as a criterion in the classification of aerobic actinomycetes. *Int J Syst Bacteriol* 1970;20:435–443.
25. Staneck JL, Roberts GD. Simplified approach to identification of aerobic actinomycetes by thin-layer chromatography. *Appl Microbiol* 1974;28:226–231.
26. Collins MD, Pirouz T, Goodfellow M, Minnikin DE. Distribution of menaquinones in actinomycetes and corynebacteria. *J Gen Microbiol* 1977;100:221–230.
27. Kroppenstedt RM. Separation of bacterial menaquinones by HPLC using reverse phase (RP18) and a silver loaded Ion exchanger as stationary phases. *J Liq Chromatogr* 1982;5:2359–2367.
28. Schleifer KH, Kandler O. Peptidoglycan types of bacterial cell walls and their taxonomic implications. *Bacteriol Rev* 1972;36:407–477.
29. Sasser M. Identification of bacteria by gas chromatography of cellular fatty acids. *USFCC Newsl* 1990;20:16.
30. William S, Feil H, Copeland A. Bacterial genomic DNA isolation using CTAB. *Sigma* 2012;50.
31. Kolmogorov M, Yuan J, Lin Y, Pevzner PA. Assembly of long, error-prone reads using repeat graphs. *Nat Biotechnol* 2019;37:540–546.
32. Vaser R, Sović I, Nagarajan N, Šikić M. Fast and accurate *de novo* genome assembly from long uncorrected reads. *Genome Res* 2017;27:737–746.
33. Tatusova T, DiCuccio M, Badretdin A, Chetvernin V, Nawrocki EP, *et al*. NCBI prokaryotic genome annotation pipeline. *Nucleic Acids Res* 2016;44:6614–6624.
34. Meier-Kolthoff JP, Göker M. TYGS is an automated high-throughput platform for state-of-the-art genome-based taxonomy. *Nat Commun* 2019;10:2182.
35. Meier-Kolthoff JP, Carbasse JS, Peinado-Olarte RL, Göker M. TYGS and LPSN: a database tandem for fast and reliable genome-based classification and nomenclature of prokaryotes. *Nucleic Acids Res* 2022;50:D801–D807.
36. Lefort V, Desper R, Gascuel O. FastME 2.0: a comprehensive, accurate, and fast distance-based phylogeny inference program. *Mol Biol Evol* 2015;32:2798–2800.
37. Alipour M, Bininda-Emonds ORP, Moret BME, Stamatakis A. How many bootstrap replicates are necessary? *J Comput Biol* 2010;17:337–354.
38. Meier-Kolthoff JP, Auch AF, Klenk H-P, Göker M. Genome sequence-based species delimitation with confidence intervals and improved distance functions. *BMC Bioinformatics* 2013;14:60.
39. Yoon S-H, Ha S, Lim J, Kwon S, Chun J. A large-scale evaluation of algorithms to calculate average nucleotide identity. *Antonie van Leeuwenhoek* 2017;110:1281–1286.
40. Wayne LG, Brenner DJ, Colwell RR, *et al*. International committee on systematic bacteriology. Report of the *ad hoc* committee on reconciliation of approaches to bacterial systematics. *Int J Syst Bacteriol* 1987;37:463–464.
41. Goris J, Konstantinidis KT, Klappenbach JA, Coenye T, Vandamme P, *et al*. DNA-DNA hybridization values and their relationship to whole-genome sequence similarities. *Int J Syst Evol Microbiol* 2007;57:81–91.
42. Chun J, Oren A, Ventosa A, Christensen H, Arahal DR, *et al*. Proposed minimal standards for the use of genome data for the taxonomy of prokaryotes. *Int J Syst Evol Microbiol* 2018;68:461–466.
43. Lee SA, Kim HS, Sang MK, Song J, Weon HY. Effect of *Bacillus mesonae* H20-5 treatment on rhizospheric bacterial community of tomato plants under salinity stress. *Plant Pathol J* 2021;37:662–672.
44. Wang X, Dai Z, Zhao H, Hu L, Dahlgren RA, *et al*. Heavy metal effects on multitrophic level microbial communities and insights for ecological restoration of an abandoned electroplating factory site. *Environmental Pollution* 2023;327:121548.
45. Zhao Y, Duan FA, Cui Z, Hong J, Ni SQ. Insights into the vertical distribution of the microbiota in steel plant soils with potentially toxic elements and PAHs contamination after 60 years operation: abundance, structure, co-occurrence network and functionality. *Sci Total Environ* 2021;786:147338.
46. Liu Z, Yang Y, Ji S, Dong D, Li Y, *et al*. Effects of elevation and distance from highway on the abundance and community structure of bacteria in soil along Qinghai-Tibet highway. *Int J Environ Res Public Health* 2021;18:13137.
47. An M, Chang D, Hong D, Fan H, Wang K. Metabolic regulation in soil microbial succession and niche differentiation by the polymer amendment under cadmium stress. *J Hazard Mater* 2021;416:126094.
48. Siebielec S, Siebielec G, Sugier P, Woźniak M, Grządziel J, *et al*. Activity and diversity of microorganisms in root zone of plant species spontaneously inhabiting smelter waste piles. *Molecules* 2020;25:5638.
49. Li S, Wu J, Huo Y, Zhao X, Xue L. Profiling multiple heavy metal contamination and bacterial communities surrounding an iron tailing pond in Northwest China. *Sci Total Environ* 2021;752:141827.
50. Zeng XY, Li SW, Leng Y, Kang XH. Structural and functional responses of bacterial and fungal communities to multiple heavy metal exposure in arid loess. *Sci Total Environ* 2020;723:138081.
51. Overbeek R, Olson R, Pusch GD, Olsen GJ, Davis JJ, *et al*. The SEED and the Rapid Annotation of microbial genomes using Subsystems Technology (RAST). *Nucleic Acids Res* 2014;42:D206–D214.
52. Aziz RK, Devoid S, Disz T, Edwards RA, Henry CS, *et al*. SEED servers: high-performance access to the SEED genomes, annotations, and metabolic models. *PLoS One* 2012;7:e48053.
53. Sayed AM, Hassan MHA, Alhadrami HA, Hassan HM, Goodfellow M, *et al*. Extreme environments: microbiology leading to specialized metabolites. *J Appl Microbiol* 2020;128:630–657.

54. Reddy S, Sinha A, Osborne WJ. Microbial secondary metabolites: recent developments and technological challenges. In: Kumar A, Singh J and Samuel J (eds). *Volatiles and Metabolites of Microbes*. London: Academic Press; 2021. pp. 1–22.
55. Al-Shaibani MM, Radin Mohamed RMS, Sidik NM, Enshasy HAE, Al-Gheethi A, *et al*. Biodiversity of secondary metabolites compounds isolated from phylum actinobacteria and its therapeutic applications. *Molecules* 2021;26:4504.
56. Blin K, Shaw S, Augustijn HE, Reitz ZL, Biermann F, *et al*. antiSMASH 7.0: new and improved predictions for detection, regulation, chemical structures and visualisation. *Nucleic Acids Res* 2023;51:W46–W50.